

N. I. Elkalashy, M. Lehtonen, H. A. Darwish, A.-M. I. Taalab and M. A. Izzularab, A Novel Selectivity Technique for High Impedance Arcing Fault Detection in Compensated MV Networks, European Transactions on Electrical Power, ETEP, in press, published online on 23 April 2007, DOI: 10.1002/etep.179.

© 2007 John Wiley & Sons

Preprinted with permission.

A novel selectivity technique for high impedance arcing fault detection in compensated MV networks

Nagy I. Elkalashy^{1*,†}, Matti Lehtonen¹, Hatem A. Darwish²,
Abdel-Maksoud I. Taalab² and Mohamed A. Izzularab²

¹*Power Systems & High Voltage Engineering, Helsinki University of Technology (TKK), Otakaari 5 I, Otaniemi, Espoo, PO Box 3000, FI-02015 HUT, Finland*

²*Faculty of Engineering, Electrical Engineering Department, Minoufiya University, Shebin El-Kom 32511, Egypt*

SUMMARY

In this paper, the initial transients due to arc reignitions associated with high impedance faults caused by leaning trees are extracted using discrete wavelet transform (DWT). In this way, the fault occurrence is localized. The feature extraction is carried out for the phase quantities corresponding to a band frequency 12.5–6.25 kHz. The detection security is enhanced because the DWT corresponds to the periodicity of these transients. The selectivity term of the faulty feeder is based on a novel technique, in which the power polarity is examined. This power is mathematically processed by multiplying the DWT detail coefficients of the phase voltage and current for each feeder. Its polarity identifies the faulty feeder. In order to reduce the computational burden of the technique, the extraction of the fault features from the residual components is examined. The same methodology of computing the power is considered by taking into account the residual voltage and current detail coefficients where the proposed algorithm performs best. Test cases provide evidence of the efficacy of the proposed technique. Copyright © 2007 John Wiley & Sons, Ltd.

KEY WORDS: arc model; DWT; initial transients; high impedance arcing faults

1. INTRODUCTION

Electrical faults due to leaning trees are common in the Nordic countries as a result of the large forest areas. These faults cannot be detected by conventional relays due to the high resistances of the trees [1].

In distribution networks, there are several earthing concepts, such as unearthed, compensated, earthed through impedance, and solidly earthed at their neutral. Compensated earthing has grown in interest and its practical applications have increased [2–3]. In this case, the earth fault current is somewhat decreased when compared to its value in a corresponding unearthed system. This is due to the parallel resonance of the inductance connected to the neutral and network earth capacitances. Therefore, traditional detectors reacting at current thresholds are no longer practical.

*Correspondence to: Nagy I. Elkalashy, Power Systems & High Voltage Engineering, Helsinki University of Technology (TKK), Otakaari 5 I, Otaniemi, Espoo, PO Box 3000, FI-02015 HUT, Finland.

†E-mail: n_elkalashy@yahoo.com

One of the protection methods for detecting earth faults in compensated networks was to short circuit the Petersen coil using a parallel resistance to enable their detection [2]. However, the coil function was not fully gained in this case. Furthermore, a complicated mechanism is required to apply such techniques. One of the main contributions of References [3–4] was based on the analysis of the variation of the relative directions of the transient residual voltages and currents which occur during earth faults in a compensated network. When a fault occurred, whatever the earthing system used, the transients of the residual current and voltage are in opposite directions in the defective section and in the same direction in the others. However, the sensitivity limit is reached for larger fault resistances. In Reference [5], a comparison of the residual current with each phase current was used to distinguish the faulty feeder using the scalar product as the means of comparison, which reduced a number of measuring devices. Another detection technique was introduced based on analyzing the variation of the system parameters and its steady state quantities [6]. Others investigated the system harmonics, such as second order, third order, even, odd, nonharmonics, high frequency spectra, and harmonic phase angle considerations [7–9]. However, such techniques are still limited by larger fault resistance, in particular resistances greater than 100 k Ω , such as the tree resistances.

In this paper, the directionality of the initial transients associated with faults due to leaning trees is analyzed for fault selectivity purposes after extracting these transients using discrete wavelet transform (DWT). It is found that fingerprints can enhance this fault detection; that is, the transients are repeated for each half cycle due to the arc reignitions after each current zero crossing. The fault localization is carried out by investigating the DWT detail d3 coefficient of the phase voltages, which in our case corresponds to the frequency band 12.5–6.25 kHz. The sum over one power cycle is computed for the setting aim. The DWT detail coefficients of the phase currents and voltages are multiplied together. Then a summation is computed over a period of two power cycles to estimate its polarity. This polarity is used as the directionality condition and it can discriminate between the healthy and faulty feeders. However, this technique is applied on three-phase quantities (voltages and currents). To reduce the algorithm computations, the proposed technique is applied to residual voltage and currents and a better performance is gained. A practical 20 kV compensated network is simulated in ATP/EMTP and ATPDraw is used as the graphical interface. The fault model is incorporated in the network and the associated arc is implemented using the universal arc representation.

2. PROPOSED TECHNIQUE PRINCIPLES

The proposed technique mainly depends on DWT for the fault detection, as depicted in Figure 1. At each measuring node, phase voltages and feeder phase currents are measured. The fault features are extracted using DWT. The absolute sum of the phase voltage detail d3 coefficient over one cycle period of the power frequency is estimated for fault detection purposes. A threshold value of 1.0 is suggested to discriminate the fault features from measurement noise, as described in Subsection 4.1. Considering the special nature of faults due to leaning trees, a timer is used for determining the fault period to enhance the fault security. It can be implemented using a sample counter. Under certain circumstances controlled by wind speeds, the tree can move towards and away from the electrical network and the fault features can be repeated several times. Therefore, a counter can be added and used to determine a number of fault events.

In order to determine the faulty feeder, the details d3 of the voltage and current of each connected feeder are together multiplied to compute the power. Using the sum over a period of two power cycles, the power direction in the form of its polarity is utilized to identify the faulty feeder. When this power is negative, the fault occurrence is in this feeder; however, when it is positive the feeder is healthy. In a

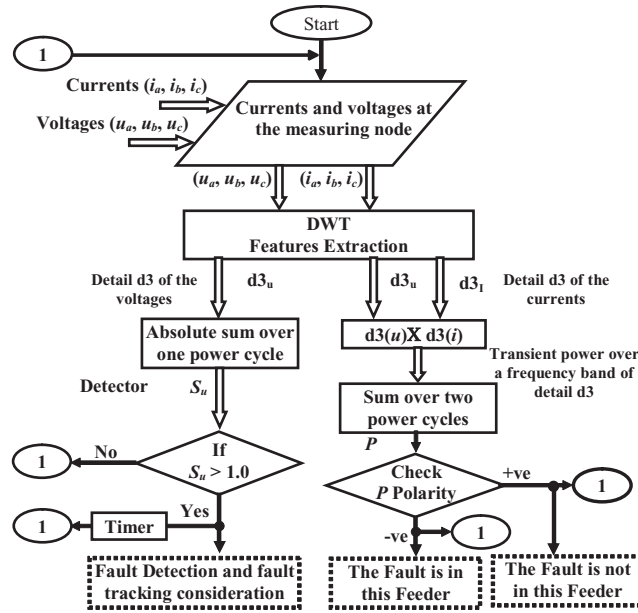


Figure 1. The proposed detection technique.

general form, when the fault features appear on the voltage details, the fault tracking process is considered. At the end of the paper, the feature extractions are carried out for the residual voltage and currents instead of the phase quantities. Therefore, the computational burden can be reduced to approximately one-third.

3. SIMULATED SYSTEM

Figure 2 shows the single line diagram of a compensated 20 kV, five-feeder distribution network simulated using ATP/EMTP, in which the processing is created by ATPDraw [10]. The feeder lines are represented using the frequency dependent JMarti model consistent with the feeder configuration given in the Appendix. The neutral of the main transformer is connected by a Petersen coil to achieve earth fault compensation. The current distributions in compensated networks during ground faults are addressed in Reference [2].

The faults due to leaning trees are modeled using two series parts: a high resistance and a dynamic arc model. For the considered trees case study, the resistance is equal to 140 kΩ and the arc is modeled according to the thermal equilibrium that is adapted as follows [1,11]:

$$\frac{dg}{dt} = \frac{1}{\tau} (G - g) \tag{1}$$

$$G = \frac{|i|}{U_{arc}} \tag{2}$$

$$\tau = Ae^{Bg} \tag{3}$$

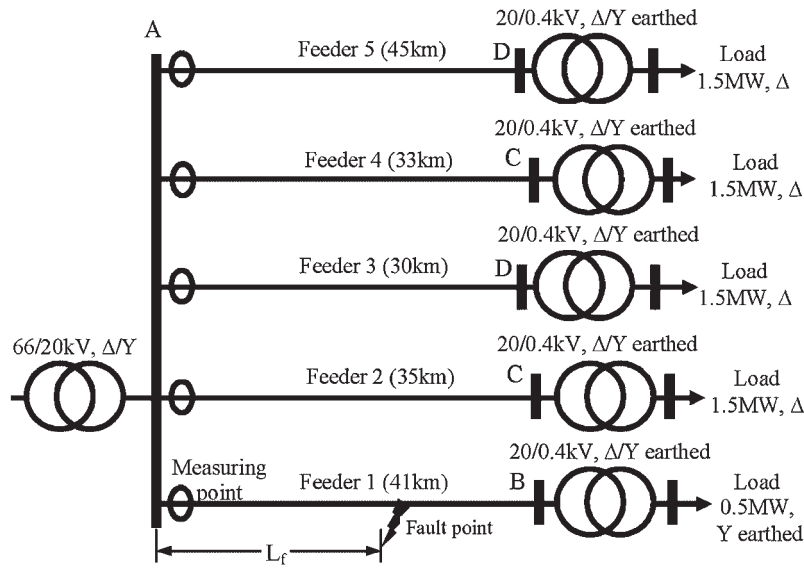


Figure 2. Simulated system for a substation energized 251 km distribution network (five feeders).

where g is the time-varying arc conductance, G is the stationary arc conductance, $|i|$ is the absolute value of the arc current, U_{arc} is a constant arc voltage parameter, τ is the arc time constant, and A and B are constants. In Reference [1], the parameters U_{arc} , A , and B were found to be 2520V, $5.6E-7$, and 395917, respectively. Considering the conductance at each zero crossing, the dielectric is represented by a variable resistance until the instant of reignition. It is represented using a ramp function of $0.5 \text{ M}\Omega/\text{ms}$ for a period of 1 ms after the zero crossing and then $4 \text{ M}\Omega/\text{ms}$ until the reignition instant.

The dynamic arc Equations (1), (2), and (3) are implemented using the universal arc representation [12]. As shown in Figure 3, the arc current is measured and transposed into the transient analysis

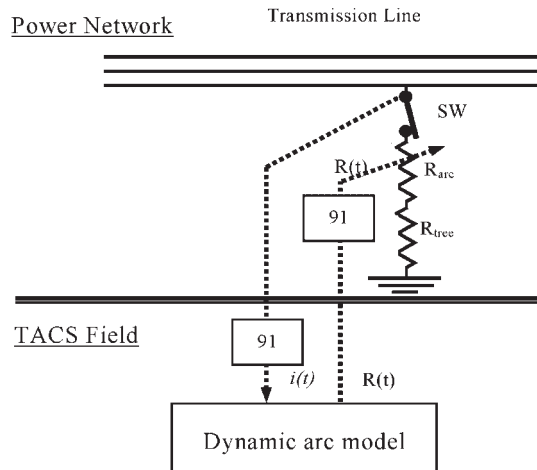


Figure 3. EMTP network of the high impedance arcing fault.

control system (TACS) field using sensor type 91 and the arc model is solved using the controlled integrator device type 58. The solved arc resistance is then sent back into the power network using the TACS-controlled resistance type 91 and so on. Control signals are generated to distinguish between arcing and dielectric periods to fulfill the reignition instant after each zero crossing.

The aforementioned medium voltage (MV) network and the fault modeling are combined in a single arrangement, as shown in the ATPDraw circuit in the Appendix. When the phase-a to ground fault occurred at the end of Feeder 1, the corresponding waveforms of the voltages and faulty feeder currents are shown in Figure 4. The fault instant is at 32 ms. The initial transients due to arc reignitions are not obvious in the waveforms, due to the tree resistance. However, the phase current and voltage waveforms contain information that correlates with the transients due to arc reignition. These initial transients were localized at different measuring nodes as will be depicted in Section 4 and also were obvious on the residual current waveforms, as will be discussed in Section 5. It is necessary to extract this information using a suitable signal processing technique such as DWT.

4. DWT-BASED FAULT DETECTION

Wavelets are families of functions generated from a single function called the mother wavelet, by means of scaling and translating operations. The scaling operation is used to dilate and compress the mother wavelet to obtain the respective high and low frequency information of the function to be

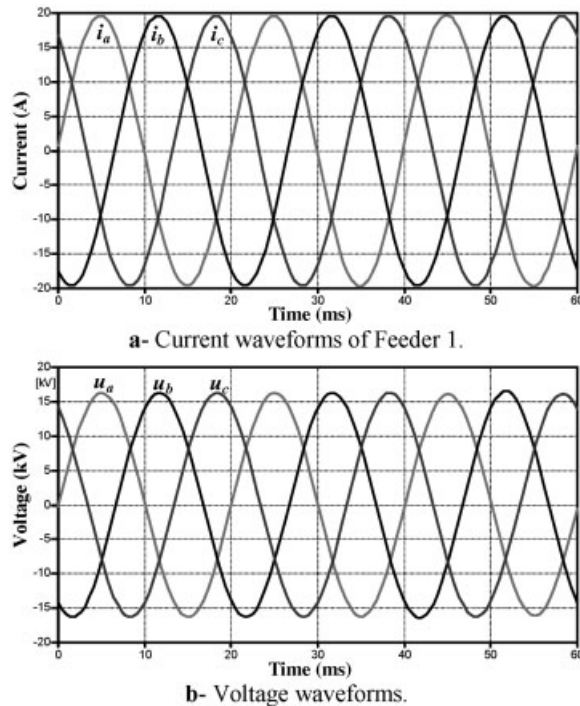


Figure 4. The waveforms when the fault occurred at the end of Feeder 1.

analyzed. Then the translation is used to obtain the time information. In this way a family of scaled and translated wavelets is created that serves as the base for representing the function to be analyzed [13]. The DWT is in the form:

$$\text{DWT}_{\psi} f(m, k) = \frac{1}{\sqrt{a_o^m}} \sum_n x(n) \psi\left(\frac{k - nb_o a_o^m}{a_o^m}\right) \quad (4)$$

where $\Psi(\cdot)$ is the mother wavelet that is discretely dilated and translated by a_o^m and $nb_o a_o^m$, respectively. a_o and b_o are fixed values with $a_o > 1$ and $b_o > 0$. m and n are integers. In the case of the dyadic transform, which can be viewed as a special kind of DWT spectral analyzer, $a_o = 2$ and $b_o = 1$. DWT can be implemented using a multi-stage filter with down sampling of the output of the low-pass filter. The practical realization of the DWT is addressed in Reference [14], where its experimental implementation was accomplished using DSP board (DSP1003), but with a reduction of its lengthy execution time.

4.1. Fault detection

Several wavelet families were tested to extract the fault features using the Wavelet toolbox incorporated into the MATLAB program [15]. Daubechies wavelet 14 (db14) is found appropriate for localizing this fault with a sampling frequency of 100 kHz. The details d3 including the frequency band 12.5–6.25 kHz have been investigated. The sampling rate can be reduced to 50 or 25 kHz but the used coefficients will be details d2 or d1, respectively. Furthermore, the sampling rate can be reduced to less than 10 kHz when considering detail d1, as concluded from testing the algorithm performance, but the test cases are not explored in the paper. However, the performance has lower gain. On the other hand, there is a practical trend for increasing the sampling rate because the speed of microprocessors is rapidly increasing. Also, signal processing implementations are continuously being advanced.

For the fault case depicted in Figure 4, fault features are extracted using DWT, as shown in Figure 5. It is obvious that the initial transients due to arc reignitions are frequently localized in the healthy and faulty phase voltage details d3. Furthermore, they are localized in the phase current details d3 of faulty and healthy feeders because there are couplings between the network phases and the earth along with the feeder lengths. Even though these transients are generated due to arc reignitions, they are controlled not only by the fault characteristics but also by the electrical network parameters and fault locations.

Using the voltage details in preference to the current details, the absolute sum value of over a period of the power frequency is computed in a discrete form, as in References [16–17]:

$$S_U(k) = \sum_{n=k-N+1}^k |d3_U(n)| \quad (5)$$

where $S_U(k)$ means the detector in the discrete samples, which is the detail level d3_U of the phase voltage U . n is used for creating a sliding window covering 20 ms and N is the number of window samples. The performance of S_U for different phases is shown in Figure 6. The detectors are high not only at the starting instant of the fault occurrence but also during the fault period, which improves the protection security. However, a threshold value equal to 1.0 is suggested to discriminate between this fault case and the measurement noise. This is evident with the aid of the experimental waveforms of this fault current and voltage illustrated in Reference [1]. In this reference, the experimental waveforms were processed using DWT with the same mother wavelet db14 for comparison purposes. It was found that the fault features are extracted using the experimental data using details d3 and d4 and there is good

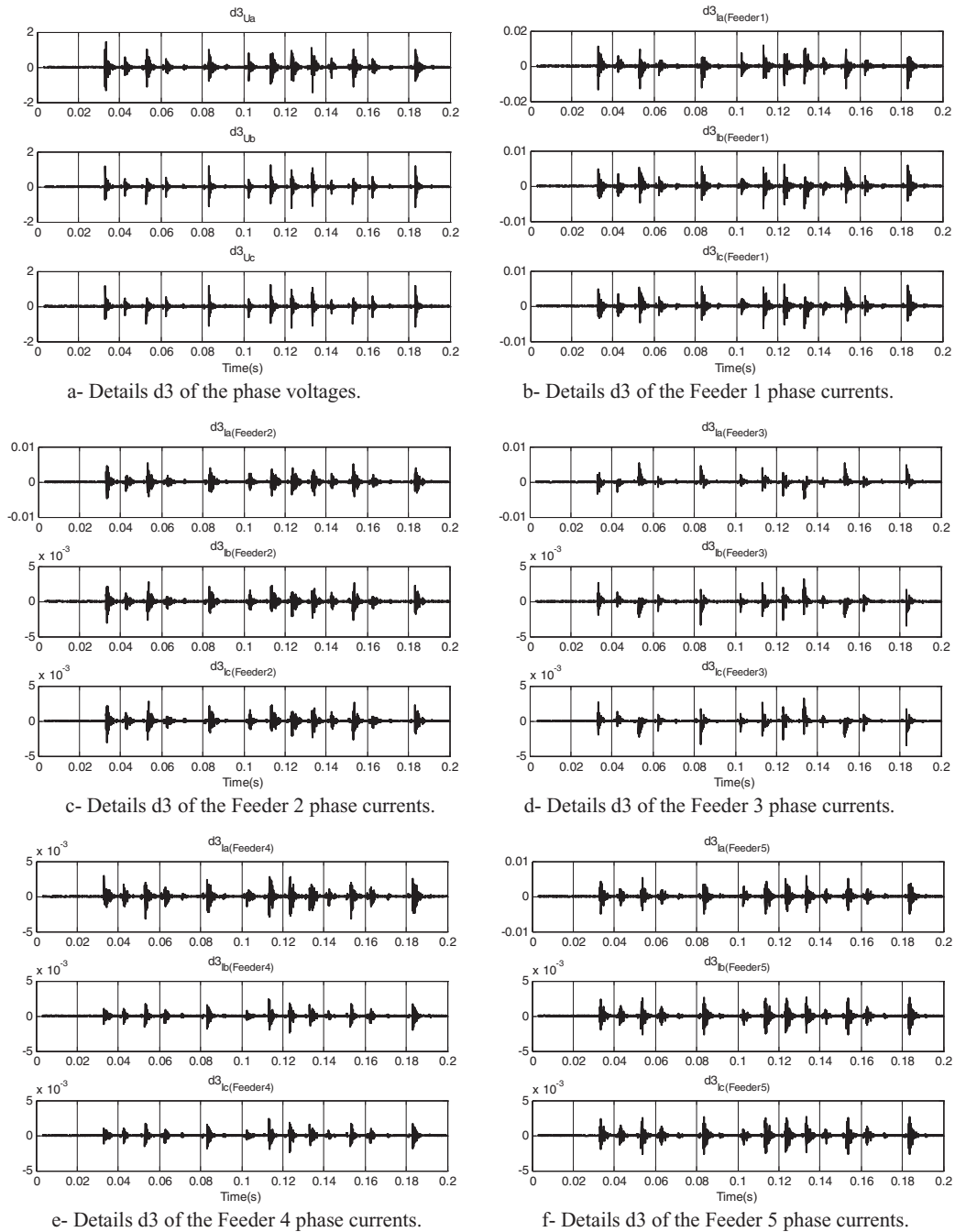


Figure 5. Details d3 of the phase voltage and current waveforms.

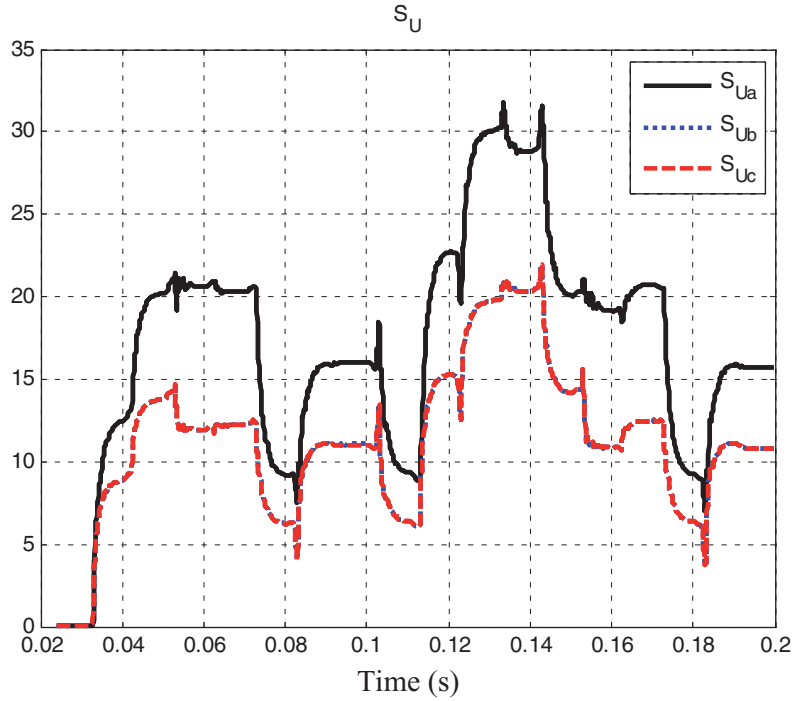


Figure 6. The detector S of the voltage details shown in Figure 5a.

agreement with the simulation results. By applying the discriminator S_U Equation (5) on the DWT details $d3$ of the experimental fault voltages in Reference [1], it was found that a threshold value of 1.0 can discriminate between the fault features and noise.

4.2. Faulty feeder discrimination

It should be noted that the aforementioned detectors can only localize the fault event; however, they cannot discriminate the faulty feeder. This shortcoming can be overcome with the aid of Figure 7, which is an enlarged view of the details $d3$ of the voltage, faulty Feeder 1 current, and the healthy feeders' currents for phase-a. It is recognizable that the details $d3$ of the voltage and currents of the healthy feeders are in-phase. However, the detail of the faulty feeder current is out of phase. This shifting can be observed by multiplying the details of the voltage ($d3_{Uj}$) and current ($d3_{Ij}$) for each phase at each feeder. It can be considered to be the harmonic-band power over the frequency range 12.5–6.25 kHz. Then its polarity is estimated using summation over a period of two power frequency cycles. As an example, this power for phase-a and for Feeder j is in the form:

$$P_{a(\text{Feeder } j)}(k) = \sum_{n=k-2N+1}^k |d3_{Ua}(n) \times d3_{Ia(\text{Feeder } j)}(n)| \quad (6)$$

where $P_{a(\text{Feeder } j)}(k)$ is used for the discrimination and its polarity is used to point out the fault point.

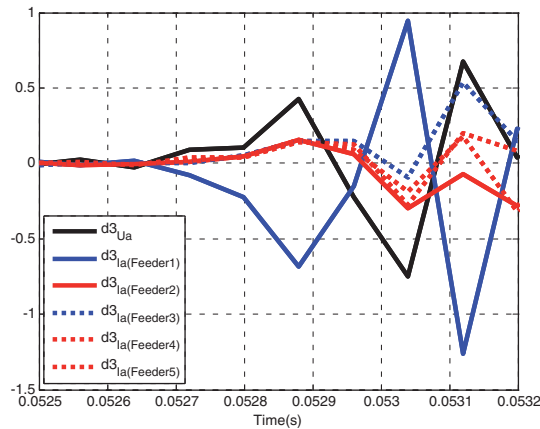


Figure 7. Enlarged view of the voltage and current details.

The discriminator performance P is shown in Figure 8. The discriminator polarity is positive for healthy feeders and negative for faulty Feeder 1 as shown in Figure 8a, where phase-a quantities are considered, and as shown in Figure 8b and c, where phase-b and c quantities are used, respectively. Therefore, this property is found to be the same for each phase, which serves to ensure the fault detection and its selectivity. However, the faulty phase is not determined. Therefore, the proposed technique can be examined considering the residual components (voltage and currents) as described in the following section and in this case the computation steps of the proposed algorithm are reduced.

5. FAULT FEATURE EXTRACTION FROM RESIDUAL WAVEFORMS

In distribution networks, the residual waveforms can be analyzed to enable detection of high impedance earth faults. They are computed as:

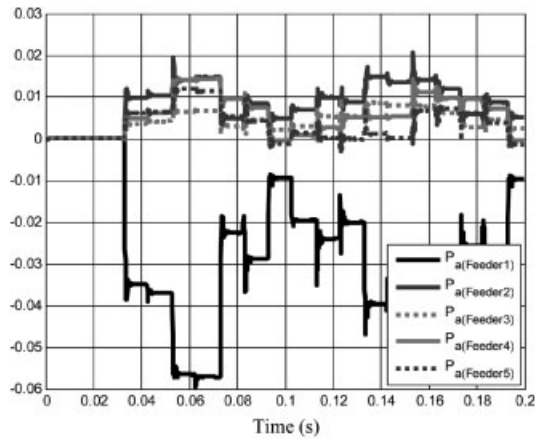
$$i_r = i_a + i_b + i_c \quad (7)$$

$$u_r = u_a + u_b + u_c \quad (8)$$

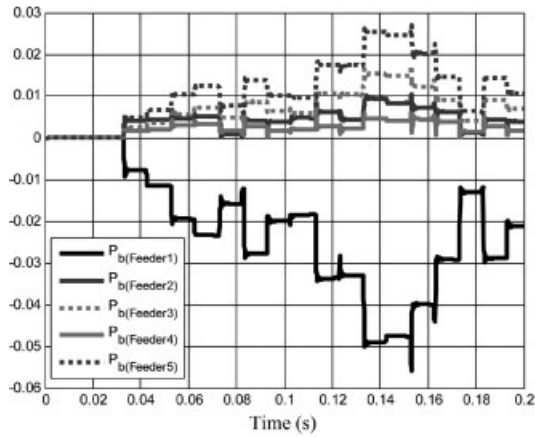
where i_r and u_r are the residual current and voltage, respectively. i_a , i_b , and i_c are the phase currents. u_a , u_b , and u_c are the phase voltages. In order to investigate these residual waveforms during the fault, Equations (7) and (8) are implemented in TACS.

Considering the same fault test case, the corresponding residual waveforms are shown in Figure 9. From the enlarged view shown in Figure 9a, the impact of the arc reignition is periodically obvious in the residual currents of both the faulty and healthy feeders. Figure 9b illustrates the residual voltages containing information related to the transients due to arc reignitions. The fault features are extracted from the residual components using DWT as shown in Figure 10, in which the same db14 is used. The flag described in Equation (5) is recalculated considering the residual voltage details and the results are shown in Figure 11. It is evident that the fault is also detected in a similar way and with higher gain.

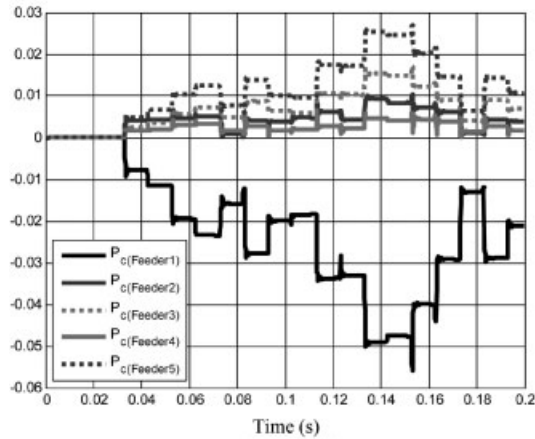
To test the proposed selectivity technique, a view of the details d3 coefficients of the residual voltage and currents is enlarged as illustrated in Figure 12. Also, it is recognizable that the details d3 of the



a- Comparison for phase-a .



b- Comparison for phase b.



c- Comparison for phase c.

Figure 8. Comparison between the discriminator P of the different feeders for each phase.

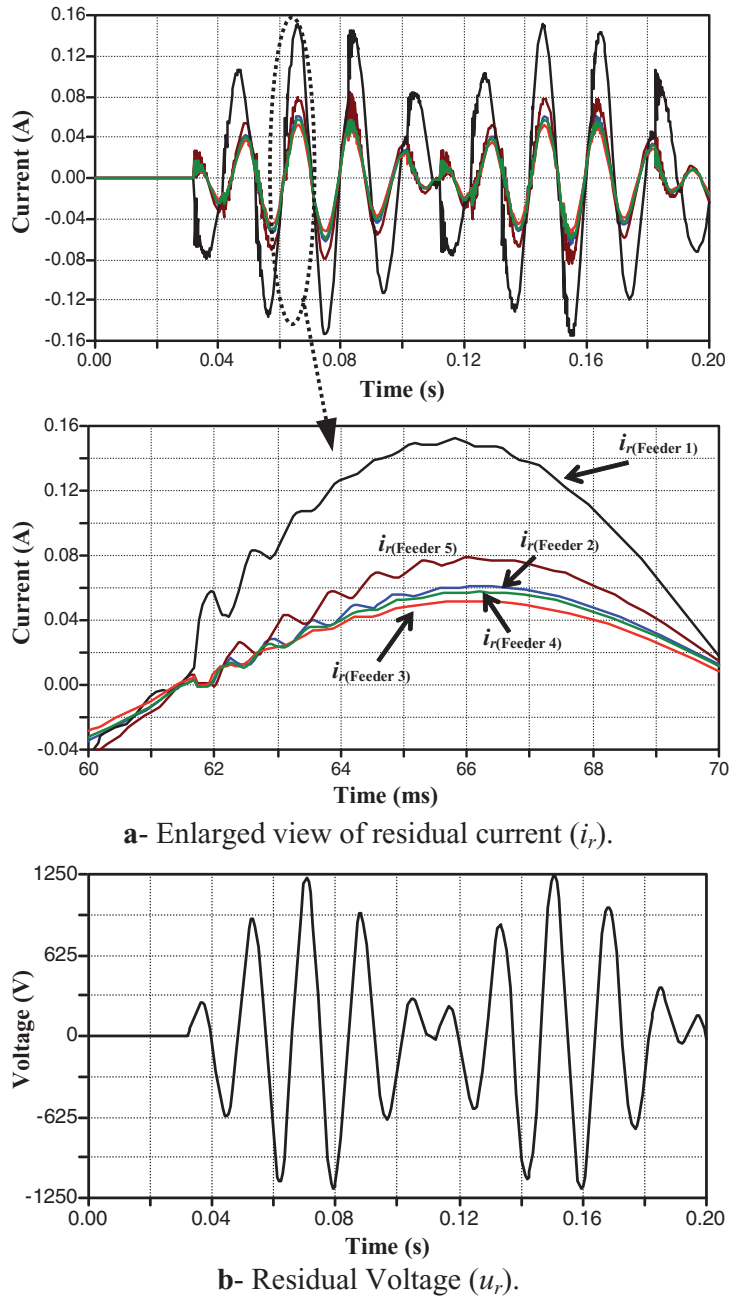


Figure 9. The residual waveforms.

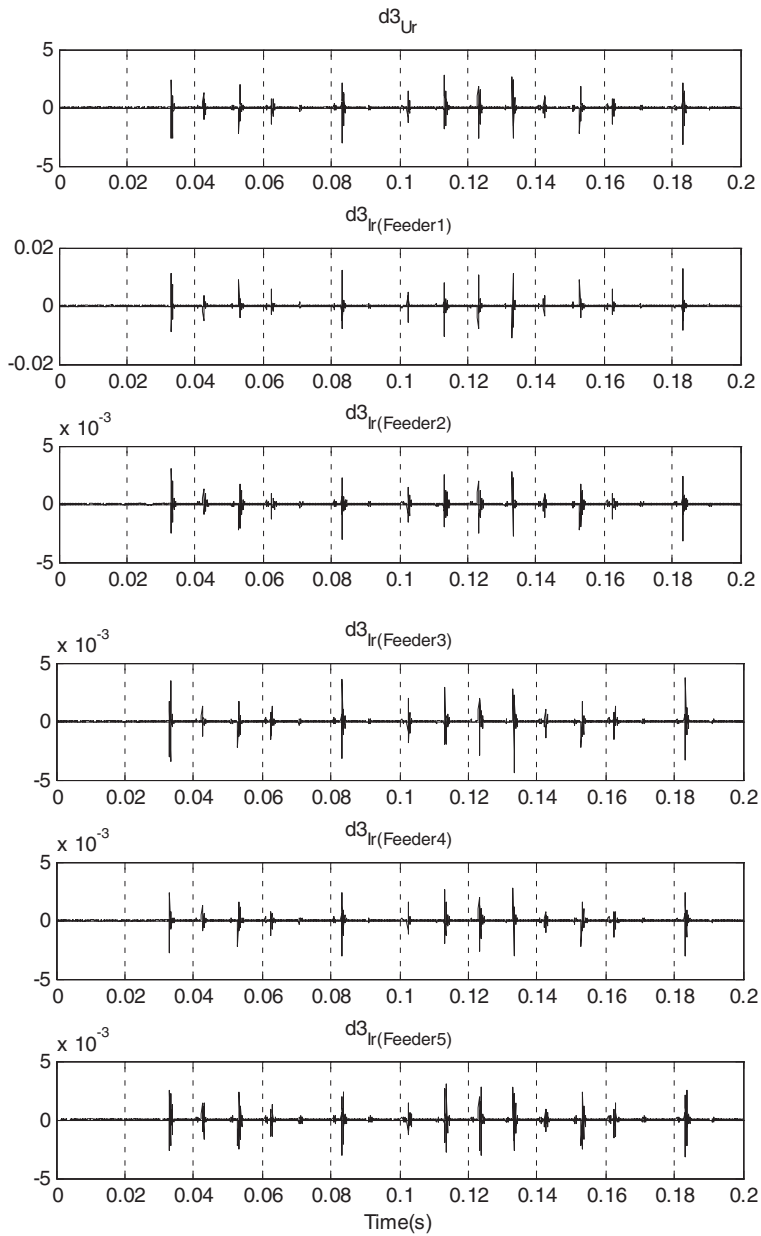


Figure 10. Details d3 of the residual voltage and feeder current waveforms.

residual voltage and currents of the healthy feeders are in-phase. However, the detail of the faulty feeder residual current is out of phase. This shifting is supervised considering a similar formula to Equation (6), but where the details of the phase quantities are replaced by the details of the residual waveforms. The discriminator performance can point out the faulty feeder as illustrated in Figure 13,

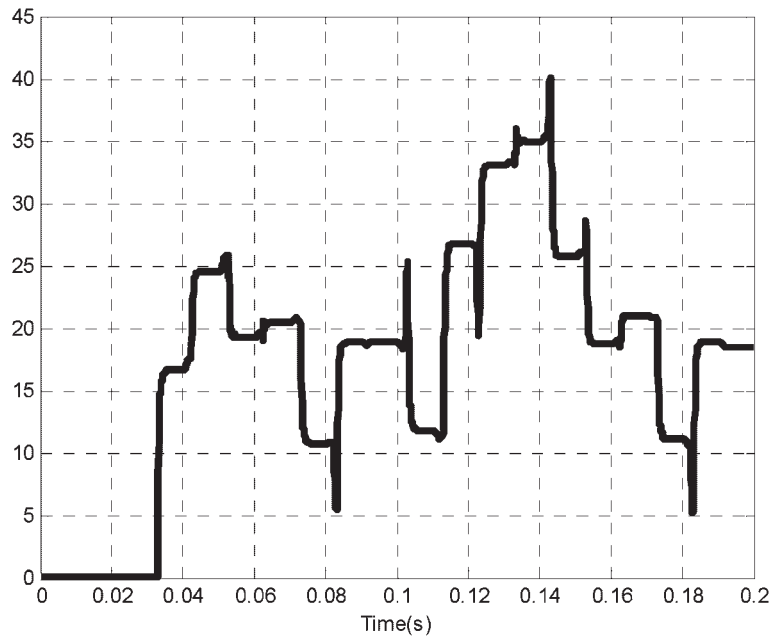


Figure 11. The detector S of the residual voltage details $d3$.

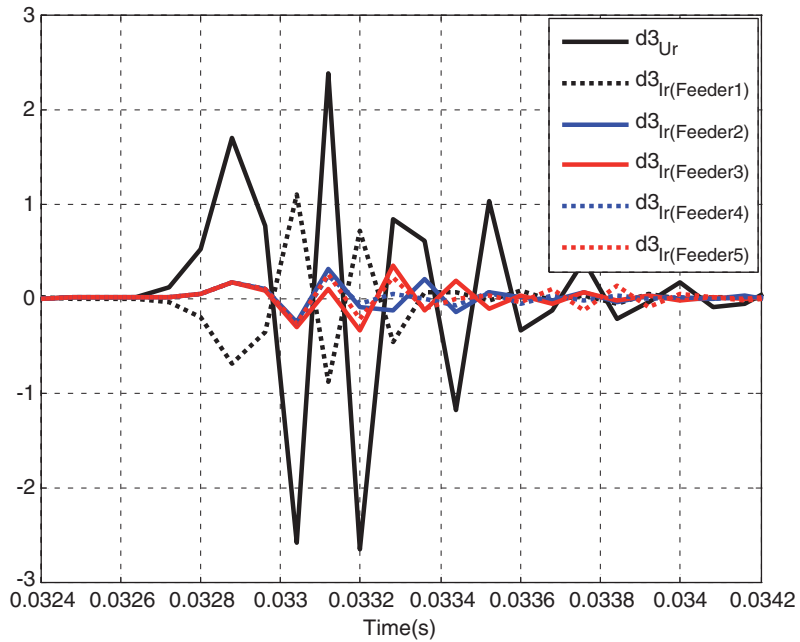


Figure 12. Enlarged view of residual voltage and current details.

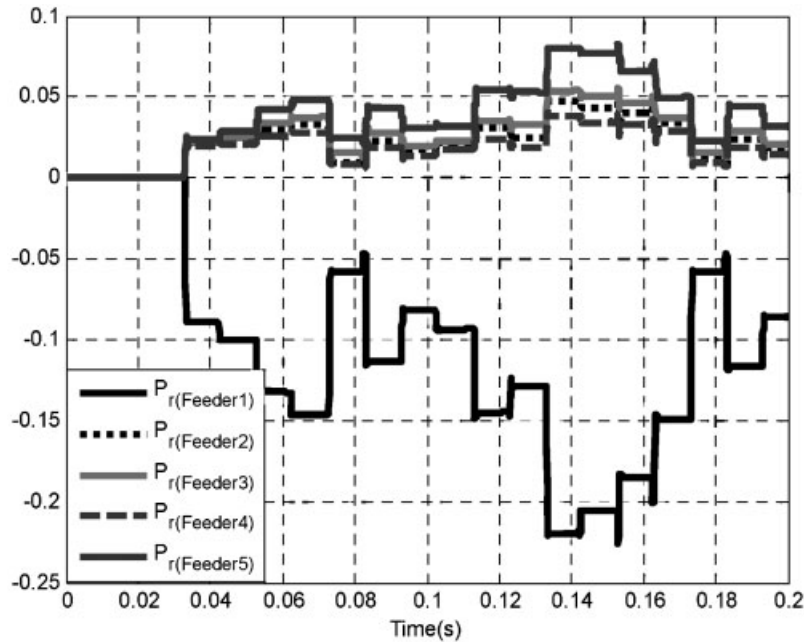


Figure 13. The discriminator P_r to determine the faulty feeder.

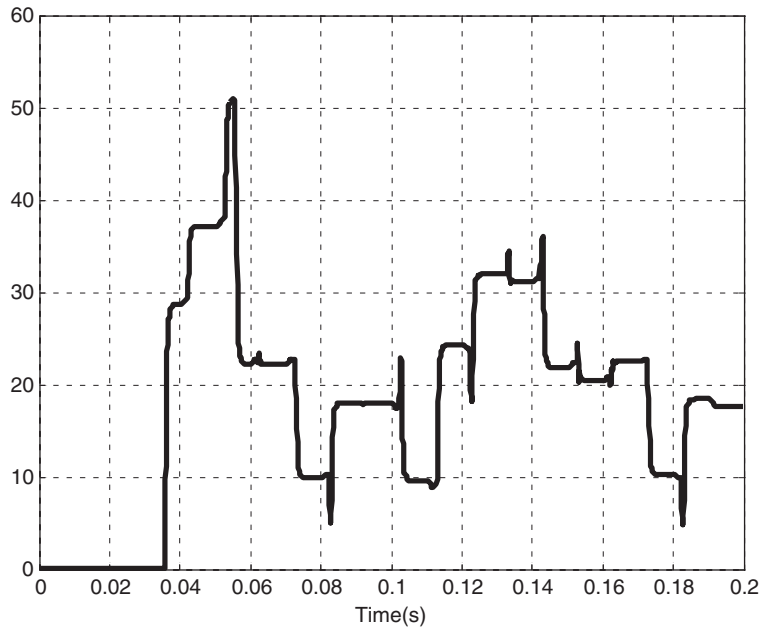
where its polarity is positive for healthy feeders and negative for the faulty feeder. By comparing the results shown in Figure 8 with those depicted in Figure 13, the performance of the proposed selectivity technique is more readable when it is applied using the residual waveforms.

The proposed detection and selectivity technique is further evaluated considering a second set of fault conditions, in which the fault distance is changed to L_f equal to 5 km and the fault instant is at 35 ms. The corresponding performance of the proposed detector and discriminator during these fault conditions is shown in Figure 14a and b, respectively. Figure 15 confirms the performance when a third fault case is considered, where the fault instant is changed to 30 ms and Feeders 1, 3, and 4 are unloaded.

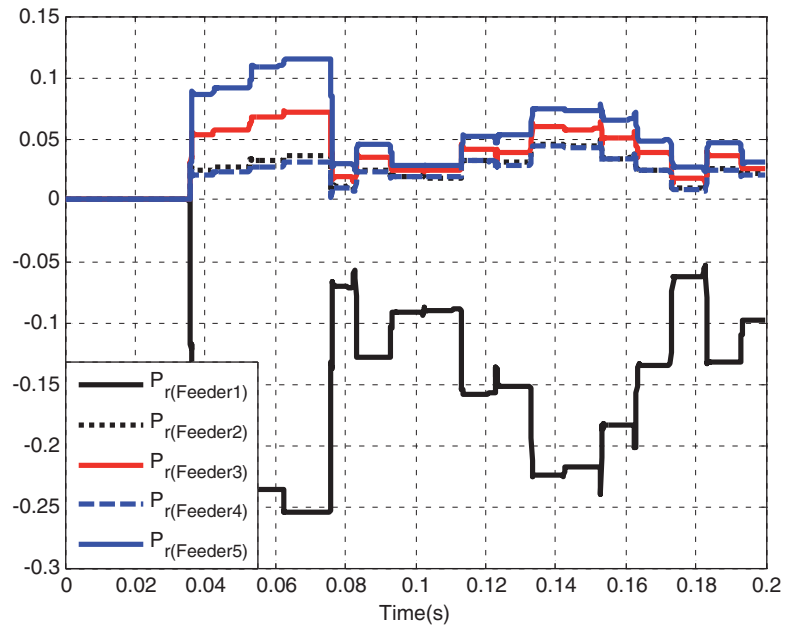
The proposed technique may respond to transients generated due to switching, such as adding or removing a feeder. However, such transients are only created at the disturbance instant without repetition after each zero crossing and the proposed detector will respond only for one power cycle. This point is useful for discriminating between switching and high impedance faults [17]. Another issue is that the proposed technique response can be blocked by a blocking signal from the circuit breaker operation. For example, if the breaker interrupts or connects a feeder, the breaker will send a signal to block the detection function for a period of one power cycle. These two latter points will enhance the fault detection security.

6. CONCLUSIONS

A novel technique for detecting a high impedance arcing fault due to a leaning tree has been introduced. The fault features have been extracted using DWT. The absolute sum over one power cycle has been



a- The detector S_{Ur}



b- The discriminator P_r .

Figure 14. The performance when the second fault case conditions are considered.

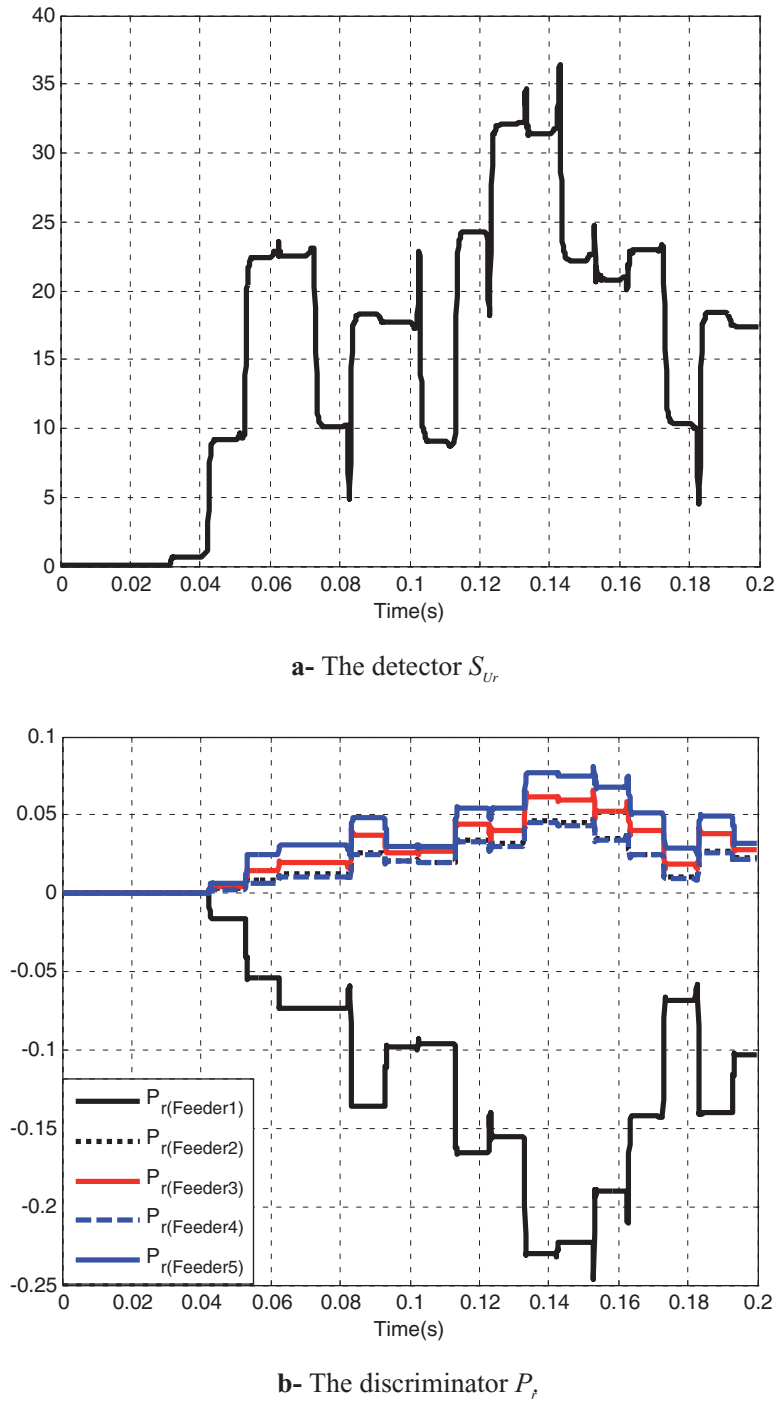


Figure 15. The performance when the third fault case conditions are considered.

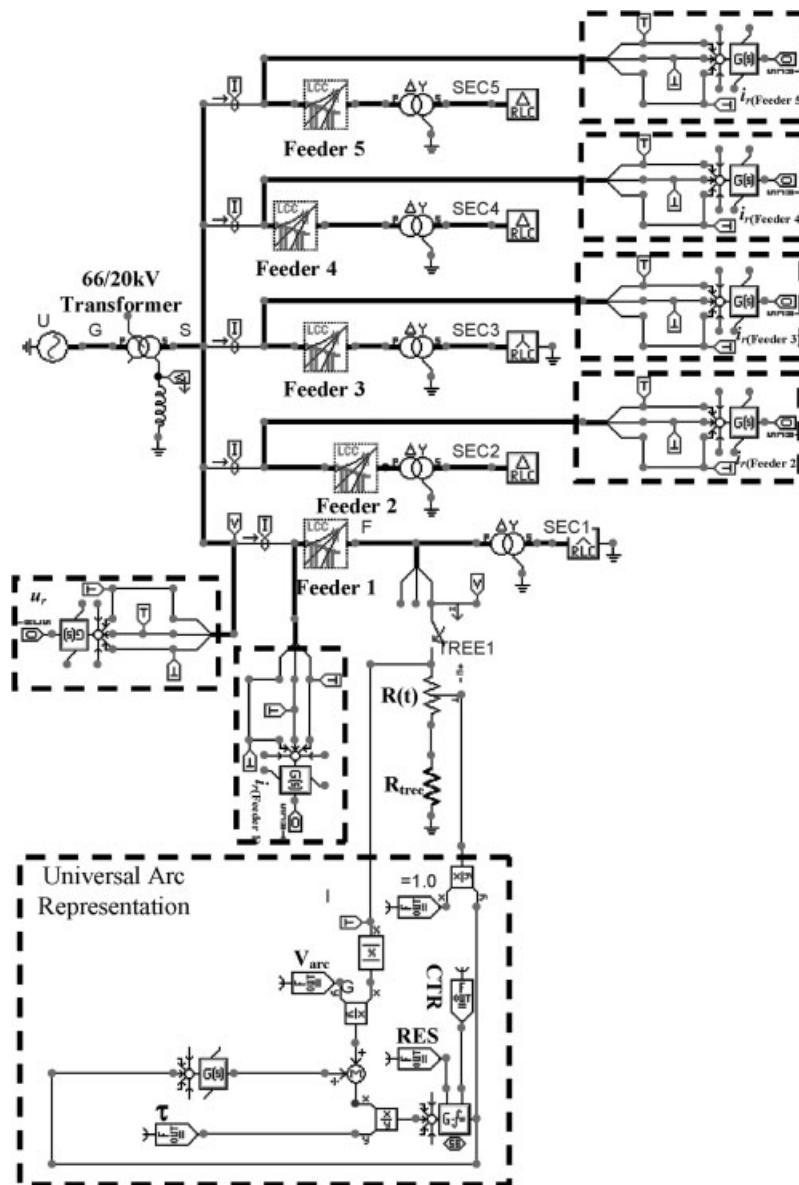


Figure 16. The ATPDraw network.

computed for the phase voltage detail d3 coefficients. The periodicity of the arc reignitions gives a specific performance for the DWT with this fault type and the results enable fault detection. The fault track has been estimated using the polarities of the power computed by multiplying the detail d3 coefficients of the voltage and current. This technique considers the residual voltage and currents instead of the phase quantities. It is found that the proposed technique is improved. Sensitive and secure detection of the faults due to leaning trees has been attained using DWT. In work to follow, an extensive

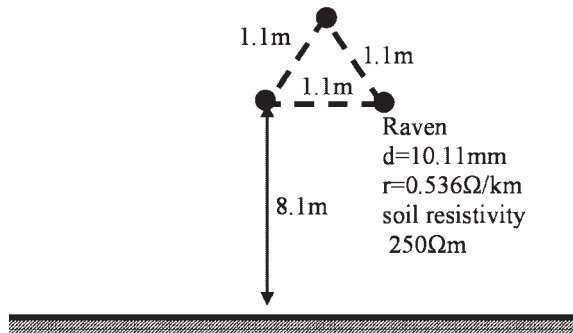


Figure 17. The feeder configuration.

investigation of the proposed technique will be carried out on a wide range of measurements gathered from different locations in the network using wireless sensors.

7. LIST OF SYMBOLS AND ABBREVIATIONS

a_o^m	dilation
a_o and b_o	fixed values with $a_o > 1$ and $b_o > 0$
A and B	constants
g	time-varying arc conductance
G	stationary arc conductance
$ i $	absolute value of the arc current
i_r	residual current
i_a, i_b, i_c	phase currents
m and n	integers
n	counter for carrying out a sliding window covering 20 ms
$nb_o a_o^m$	translation
N	number of samples
P	power computed by multiplying the DWT detail coefficients of the voltage and current and then averaging over two power cycles
$S_U(k)$	the detector in discrete samples
U_{arc}	a constant arc voltage parameter
u_r	residual voltage
u_a, u_b, u_c	phase voltages
$\psi(\cdot)$	mother wavelet
τ	arc time constant
ATP	alternative transient program
db14	Daubechies wavelet 14
DWT	discrete wavelet transform
EMTP	electromagnetic transient program
MV	medium voltage
TACS	transient analysis control system

APPENDIX

Figure 16 illustrates the considered ATPDraw network. It contains the MV network, the universal arc representation, and the residual current and voltage waveforms described by Equations (7) and (8), respectively. The feeders are represented using a frequency dependent JMarti model. Their configuration is shown in Figure 17.

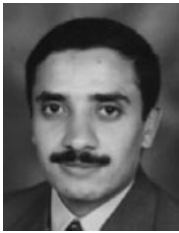
ACKNOWLEDGEMENTS

The authors gratefully acknowledge the discussions with Mr. Abdelsalam Elhafar and Mr. John Millar.

REFERENCES

1. Elkalashy N, Lehtonen M, Darwish H, Izzularab M, Taalab A. Modeling and experimental verification of a high impedance arcing fault in MV networks. *IEEE Transactions on Dielectric and Electrical Insulation* (in press).
2. Lehtonen M, Hakola T. Neutral earthing and power system protection. Earthing solutions and protective relaying in medium voltage distribution networks. ABB Transmit Oy, FIN-65101 Vassa, Finland, 1996.
3. Grima T, Flatermeier J. A new generation of materials for medium voltage compensated neutral networks. *14th International Conference and Exhibition on Electricity Distribution, CIRED, IEE Conference*, Birmingham, 2–5 June 1997.
4. Druml G, Kugi A, Seifert O. A new directional transient relay for high ohmic earth faults. *17th International Conference and Exhibition on Electricity Distribution, CIRED, IEE Conference*, Barcelona, 12–15 May 2003.
5. Assef Y, Bastard P, Meunier M. Artificial neural networks for single phase fault detection in resonant grounded power distribution systems. *IEEE Transmission and Distribution Conference*, Los Angeles, 15–20 September 1996.
6. Leitloff V, Feuillet R, Griffel D. Detection of resistive single-phase earth faults in a compensated power-distribution system. *European Transactions on Electrical Power* 1997; **7**(1):65–73.
7. Wai D, Yibin X. A novel technique for high impedance fault identification. *IEEE Transactions on Power Delivery* 1998; **13**(3):738–744.
8. Russell B, Benner C. Arcing fault detection for distribution feeders: security assessment in long term field trials. *IEEE Transactions on Power Delivery* 1995; **10**(2):676–683.
9. Jeerings D, Linders J. Unique aspects of distribution system harmonics due to high impedance ground faults. *IEEE Transactions on Power Delivery* 1990; **5**(2):1086–1094.
10. Prikler L, Hoildalen H. ATPDraw users' manual. SINTEF TR A4790, November 1998.
11. Kizilcay M, Pniok T. Digital simulation of fault arcs in power systems. *European Transactions on Electrical Power* 1991; **4**(3):55–59.
12. Darwish H, Elkalashy N. Universal arc representation using EMTP. *IEEE Transactions on Power Delivery* 2005; **2**(2):774–779.
13. Solanki M, Song Y, Potts S, Perks A. Transient protection of transmission line using wavelet transform. *Seventh International Conference on Developments in Power System Protection, (IEE)*, 9–12 April 2001; pp. 299–302.
14. Darwish HA, Farouk MH, Taalab AI, Mansour NM. Investigation of real-time implementation of DSP-based DWT for power system protection. *IEEE/PES Transmission and Distribution Conference and Exposition*, 21–26 May 2006, Dallas, Texas, USA.
15. *Wavelet Toolbox for MATLAB*, Math Works 2005.
16. Haung J, Shen C, Phoong S, Chen H. Robust measure of image focus in the wavelet domain. *International Symposium on Intelligent Signal Processing and Communication Systems, ISPACS2005*, 13–16 December 2006, Hong Kong.
17. Kim C, Kim H, Ko Y, Byun S, Aggarwal K, Johns A. A novel fault-detection technique of high-impedance arcing faults in transmission lines using the wavelet transform. *IEEE Transactions on Power Delivery* 2002; **17**(4):921–929.

AUTHORS' BIOGRAPHIES



Nagy I. Elkalashy (S'06) was born in Quesna, Egypt on 4 August 1974. He received his B.Sc. (with first class honors) and M.Sc. degrees from the Electrical Engineering Department, Faculty of Engineering, Shebin El-Kom, Menoufiya University in 1997 and 2002, respectively. Currently, he is working toward the Ph.D. degree at Power Systems and High Voltage Engineering, Helsinki University of Technology (TKK), Finland, under joint supervision with Menoufiya University. His research interests are high impedance fault detection, power system transient studies including AI, EMTP simulation, and switchgear (E-mail: nagy.elkalashy@hut.fi, n_elkalashy@yahoo.com).



Matti Lehtonen (1959) was with VTT Energy, Espoo, Finland from 1987 to 2003, and since 1999 has been a professor at the Helsinki University of Technology, where he is now head of Power Systems and High Voltage Engineering. Matti Lehtonen received both his Master's and Licentiate degrees in Electrical Engineering from Helsinki University of Technology in 1984 and 1989, respectively, and the Doctor of Technology degree from Tampere University of Technology in 1992. His main activities include power system planning and asset management, power system protection including earth fault problems, harmonic related issues and applications of information technology in distribution systems (E-mail: Matti.Lehtonen@hut.fi).



Hatem A. Darwish (M'06-SM'06) was born in Quesna, Egypt on 13 September 1966. He received his B.Sc. (honors), M.Sc., and Ph.D. degrees in Electrical Engineering, Menoufiya University, Egypt in 1988, 1992, and 1996, respectively. From 1994 to 1996, he completed his Ph.D degree at the Memorial University of Newfoundland (MUN), St. John's, Canada, based on joint supervision with Menoufiya University. He has been involved in several pilot projects for the Egyptian industry for the design and implementation of numerical relays, SCADA, fault location in MV feeders, distribution management systems, protection training packages, and relay coordination. His interests are in digital protection, signal processing, system automation, and EMTP ac/dc simulation, and switchgear (E-mail: h_a_darwish@yahoo.com).



Abdel-Maksoud I. Taalab (M'99-SM'03) received his B.Sc. degree in 1969, in Electrical Engineering from Menoufiya University, Egypt, and M.Sc. and Ph.D. degrees from Manchester University, U.K. in 1978 and 1982, respectively. In the same year as his graduation, he was appointed to be an Assistant Professor at the Menoufiya University. He joined the GEC Company in 1982. He is now a full professor at the department of Electrical Engineering, Faculty of Engineering, and Vice Dean of the Desert Environment Institute, Menoufiya University. His interests are in HVDC transmission systems, power system protection, and power electronics applications (E-mail: taalab3@yahoo.com).



Mohamed A. Izzularab was born in Tanta, Egypt in 1950. He received his B.Sc. degree in Electrical Engineering from Menoufiya University, Egypt in 1973. He was awarded the M.Sc. degree from Elmansoura University in 1978 and Dr Ing degree from I.N.P.T. Toulouse, France in 1983. He was also awarded the D.Sc. in Electrical Engineering from Paul Sabatier University Toulouse, France in 1987. He obtained the Cigre Award for the best-applied research for the year 1998. Dr Izzularab is the Vice President, Minoufiya University (E-mail: mizzularab@yahoo.com).